DYNAMICS OF MULTI-KINKS IN THE PRESENCE OF WELLS AND BARRIERS

Stephen W. Goatham[†], Lucy E. Mannering[‡], Rebecca Hann[§]
Steffen Krusch[¶]

School of Mathematics, Statistics and Actuarial Science, University of Kent
Canterbury CT2 7NF, United Kingdom

(Received June 30, 2011)

Sine-Gordon kinks are non-dispersive solutions in a much studied integrable system. Recent studies on sine-Gordon kinks with space-dependent square-well-type potentials have revealed interesting dynamics of a single kink interacting with wells and barriers. In this paper, we study a class of smooth space-dependent potentials and discuss the dynamics of one kink in the presence of different wells. We also present values for the critical velocity for different types of barriers. Furthermore, we study two kinks interacting with various wells and describe interesting trajectories such as double-trapping, kink knock-out and double-escape.

DOI:10.5506/APhysPolB.42.2087
PACS numbers: 11.10.Lm, 05.45.Yv

1. Introduction

Topological solitons arise in many classical field theories [1]. One of the simplest systems to admit topological solitons is the sine-Gordon model. In fact, this $(1+1)$ dimensional model gives rise to a variety of different solutions such as wave-like solutions, topological soliton solutions usually referred to as kinks, as well as breather and kink–antikink solutions which do not carry a topological charge. The sine-Gordon model is described by the Lagrangian density

$$\mathcal{L} = \frac{1}{2}\left(\frac{\partial\phi}{\partial t}\right)^2 - \frac{1}{2}\left(\frac{\partial\phi}{\partial x}\right)^2 - \lambda\left(1-\cos\phi\right) , \tag{1}$$

[†] swg3@kent.ac.uk
[‡] lm231@kent.ac.uk
[§] rebeccahann@tiscali.co.uk
[¶] S.Krusch@kent.ac.uk

where $\phi(x,t)$ is a real scalar field and λ is a coupling constant. Applying the standard variational principle leads to the field equation

$$\frac{\partial^2\phi}{\partial t^2} - \frac{\partial^2\phi}{\partial x^2} + \lambda \sin\phi = 0\,. \tag{2}$$

This so-called sine-Gordon equation has applications in a large number of areas of physical and bio-physical interest, including the Josephson effect [2], nuclear physics [3], non-linear optics [4], ferromagnetic spin chains [5] and wave propagation in brain microtubules [6], amongst others. Taking a spin chain in the easy plane model of a ferromagnet as an example, λ is determined by the strength of the magnetic field, which occurs in a direction in the (x,y) easy plane (see [5] for details). When this system becomes inhomogeneous, that is the magnetic field has a z-dependence, then the corresponding parameter λ is also space-dependent. The Bloch equation describing the system still leads to a sine-Gordon equation, and solitons can still occur. We will not discuss physical interpretations further. In this paper, we shall be interested in the sine-Gordon model with parameter λ, which, as a function of space, is of the form of a smooth well or barrier. For our system, λ will be positive and, far away from the origin, very close to unity.

The interaction of a sine-Gordon soliton with a potential obstacle was investigated by Fei *et al.* [7]. The authors investigated a kink incident on a point defect and found a novel behaviour in which, for certain incoming velocities, the kink is reflected backwards, due to its interaction with the defect. Many of the results in [7] were explained by Goodman and Haberman [8] in terms of a two-bounce resonance model. The interaction of a kink with a kink pinned by a point defect has been discussed in [9], see also [10] for a review on related soliton dynamics.

In [11] Piette and Zakrzewski investigated a sine-Gordon kink interacting with a potential with a space-dependent term in the form of a rectangular well. The authors found that back-reflection for some incoming velocities also arises for this system and gave two effective models to account for this phenomenon. Soliton interactions with rectangular wells have also been discussed for various other soliton systems [12, 13, 14, 15, 16, 17, 18]. A kink interacting with a smooth well is discussed in [19] in terms of the sine-Gordon model and in [20] for the $\lambda\phi^4$ model. While these papers address the dynamics of a kink interacting with a well, multi-kinks interacting with extended wells have so far not been investigated.

In this paper, Section 2 gives a review of sine-Gordon kinks. Then Section 3 introduces a two-parameter family of space-dependent potentials which include a variety of wells and barriers. In Section 4, the results of simulations of the dynamics of a single kink interacting with a particular well are given. We also calculate critical velocities for barriers and compare

numerical results to an analytic approximation. In Section 5, the dynamics of a moving kink incident on a well with another initially at rest in the well are presented. The paper also gives plots of the scattering data for 1-kink and 2-kink systems with two different types of wells, these are discussed at the end of Section 5. The paper ends with a conclusion.

2. Sine-Gordon kinks

In this section, we recall some basic facts about sine-Gordon kinks and set up our notation.

The energy of a static sine-Gordon kink is

$$E = \int_{-\infty}^{\infty} \left(\frac{1}{2} \left(\frac{d\phi}{dx} \right)^2 + \lambda \left(1 - \cos \phi \right) \right) dx \,. \tag{3}$$

One can also define a super potential, W, given by

$$\frac{1}{2} \left(\frac{dW}{d\phi} \right)^2 = \lambda \left(1 - \cos \phi \right) \,. \tag{4}$$

The energy (3) can then be rewritten in terms of two integrals

$$E = \frac{1}{2} \int_{-\infty}^{\infty} \left(\frac{d\phi}{dx} \mp \frac{dW}{d\phi} \right)^2 dx \pm \int_{\phi(-\infty)}^{\phi(\infty)} dW \,. \tag{5}$$

For a minimum energy soliton, we obtain the Bogomolny equations

$$\frac{d\phi}{dx} = \pm \frac{dW}{d\phi} \,, \tag{6}$$

where the $\pm$ sign gives a kink or antikink. Substituting the solution of (4) into (6) gives the kink field

$$\phi(x) = 4 \arctan \left(\exp \left(\sqrt{\lambda} (x - X) \right) \right) \,, \tag{7}$$

where X is a constant of integration and corresponds to the position of the kink. The energy can then be evaluated to be $8\sqrt{\lambda}$, so one has the Bogomolny bound

$$E \geq 8\sqrt{\lambda} \,. \tag{8}$$

Since the Lagrangian density (1) is Lorentz invariant, a boost can be applied to (7) to give a moving kink with field configuration

$$\phi = 4 \arctan \left(\exp \left(\gamma \left(x - vt - X \right) \right) \right) \,, \tag{9}$$

where v is the velocity of the kink, with $-1 < v < 1$, and $\gamma = \frac{1}{\sqrt{1-v^2}}$ is the Lorentz factor, and we have set $\lambda = 1$ for simplicity. There is a topological charge N associated with a sine-Gordon kink given by

$$N = \frac{1}{2\pi} \int_{-\infty}^{\infty} \frac{d\phi}{dx} dx \,. \tag{10}$$

At $x = \pm\infty$ the field ϕ needs to minimize the potential energy in (3), hence we choose $\phi(-\infty) = 0$ and $\phi(\infty) = 2\pi N$. Therefore, equation (10) clearly takes integer values. For charge N the Bogomolny bound becomes

$$E \geq \left| \int_{\phi(-\infty)=0}^{\phi(\infty)=2\pi N} dW \right| = 8|N|\sqrt{\lambda} \,. \tag{11}$$

For the case of multi-kinks this bound cannot be saturated as there is a repulsive force between two static kinks. Indeed, in [3] Perring and Skyrme show that the asymptotic interaction energy of two sine-Gordon kinks is given by

$$E_{\text{int}} = 32\sqrt{\lambda} e^{-\sqrt{\lambda} R} \,, \tag{12}$$

where R is the separation between the kinks.

As well as being Lorentz invariant, the sine-Gordon model is also fully integrable (see [21] for a review of integrable systems). Therefore, it has the feature that solution generating techniques, such as the Bäcklund transformation, are applicable (see *e.g.* [22]). For $N = 2$ this transformation can be used to obtain the field

$$\phi = 4 \arctan \left(\frac{v \sinh\left(\frac{x - vt}{1-v^2}\right)}{\cosh\left(\frac{vt - v^2 x}{1-v^2}\right)} \right) . \tag{13}$$

This describes two individual kinks, one static at negative infinity in time and the other travelling with speed v at this instant. The field configurations of the kinks gradually approach each other with time and the solitons interact. For simplicity, we have set $\lambda = 1$ in formula (13).

In the sine-Gordon model there is also a breather solution, which exists in the charge zero sector and can be interpreted as a kink–antikink bound state. A solution that is a bound state of a breather and kink, the sine-Gordon wobble, is described in [23]. These solutions show interesting behaviour when they are interacting with square wells [16, 17].

3. A class of space-dependent potentials

In the following, we describe a class of space-dependent potentials, where the coupling constant λ in (2) becomes space-dependent. Square-well-type potentials have been discussed for example in [11]. These have the disadvantage that they are not smooth. Here, we propose a smooth two-parameter family of barriers and wells, with the additional advantage that there is an analytic solution for a static kink located at the centre of the barrier or well. Figure 1 displays the wells which we study in this paper, and figure 2 shows a selection of barriers.

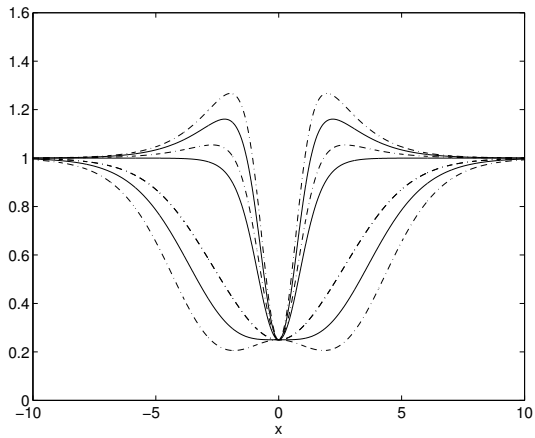

Fig. 1. Wells with $\lambda(0) = \frac{1}{4}$ for various values of a and b. Detailed scattering experiments have been performed on the wells displayed with solids lines. These are the quartic well ($a = \frac{5\sqrt{5}}{32}$, $b = \frac{3\sqrt{5}}{32}$), a narrow well without humps ($a = 0$, $b = \sqrt{10}/4$) and a generic well with humps ($a = -0.25$, $b = 1.126166088$). Some other examples of wells are displayed in dotted lines, for example the double well ($a = \frac{3}{8}$, $b = \frac{1}{8}$).

The static kink (7) located at $x = X$ solves the static field equations

$$\partial_{xx}\phi - \lambda \sin\phi = 0\,, \tag{14}$$

for constant λ. By allowing λ to depend on x we can solve equation (14) for $\lambda(x)$ for any given static field configuration. However, *a priori* it is not clear whether such a $\lambda(x)$ is non-singular. We will show in the following that we can find a two parameter family of kinks located at $x = 0$ which solves the static field equations (14) such that $\lambda(x)$ is non-singular for all real values of x. The kinks are given by

$$\phi(x) = \pi + 2\arctan\left(ax + b\sinh(x)\right) \tag{15}$$

provided that we set

$$\lambda(x) = \frac{n_2 x^2 + n_1 x + n_0}{d_3 x^3 + d_2 x^2 + d_1 x + d_0}\,, \tag{16}$$

where

$$\begin{aligned} n_2 &= -a^2 b \sinh(x)\,, \\ n_1 &= 2a\left(b^2 + a^2 + 2ab\cosh(x)\right)\,, \\ n_0 &= b\sinh(x)\left(b^2 + 2a^2 - 1 + 4ab\cosh(x) + b^2\cosh(x)^2\right)\,, \end{aligned}$$

and

$$\begin{aligned} d_3 &= a^3\,, \\ d_2 &= 3a^2 b\sinh(x)\,, \\ d_1 &= a\left(1 - 3b^2 + 3b^2\cosh(x)^2\right)\,, \\ d_0 &= b\sinh(x)\left(1 - b^2 + b^2\cosh(x)^2\right)\,. \end{aligned}$$

Note that the trivial vacuum solutions $\phi(x) \equiv 2\pi n$ also satisfy (14) for all functions $\lambda(x)$ provided n is an integer.

It is easy to see that $\lambda(x) = \lambda(-x)$ and that the map

$$(a, b) \mapsto (-a, -b) \tag{17}$$

leaves $\lambda(x)$ invariant. Physically, this means that λ is the same for a kink ($b > 0$) and an antikink ($b < 0$). In the following, we restrict our attention to kinks and set $b \geq 0$. Since the $\sinh(x)$ term dominates for large $|x|$ the parameter a can take positive and negative values provided $b > 0$. Setting $b > 0$ also guarantees that

$$\lim_{|x|\to\infty} \lambda(x) = 1\,, \tag{18}$$

which means that the kink located at X given by (7) tends to the exact solution for large $|X|$, that is when the kink is far enough away from the well. For $b = 0$, the asymptotics change. In this case,

$$\lambda(x) = \frac{2a^2}{a^2 x^2 + 1}\,, \tag{19}$$

which tends to 0 as $|x| \to \infty$. Since we want the usual sine-Gordon kink (7) to be an asymptotic solution, we only consider the case $b > 0$.

In order to determine the values of a and b for which $\lambda(x)$ is regular, we solve equation (14) for λ and obtain

$$\lambda(x) = \frac{\partial_{xx}\phi}{\sin\phi}\,. \tag{20}$$

Therefore, singularities can only occur for $\sin\phi = 0$. With our choice of $b > 0$ we have

$$-\frac{\pi}{2} < \arctan\left(ax + b\sinh(x)\right) < \frac{\pi}{2}\,, \tag{21}$$

hence, since arctan is a monotonic function and $\arctan(0) = 0$, $\lambda(x)$ can only have singularities at $g(x) = 0$, where

$$g(x) = ax + b\sinh(x)\,. \tag{22}$$

Taking the derivative of (22) leads to

$$g'(x) = a + b\cosh(x)\,. \tag{23}$$

This implies that $g'(x) > 0$ for $a+b > 0$, so that $g(x)$ is a monotonic function whose only root is $x = 0$. We can evaluate the limit

$$\lim_{x\to 0}\lambda(x) = \frac{2(a+b)^3 - b}{a+b}\,. \tag{24}$$

Hence, $\lambda(x)$ diverges for $b > 0$ and $a \to -b$. For $a + b < 0$, the function $g(x)$ has one maximum and one minimum and hence two non-trivial zeros. Generically, $\lambda(x)$ will be singular for $a + b \leq 0$.

Physical applications usually demand that $\lambda(x) > 0$. This condition is satisfied provided a satisfies the stronger inequality

$$a + b > \left(\frac{b}{2}\right)^{\frac{1}{3}}\,. \tag{25}$$

Furthermore, we are mostly interested in wells located at the origin, which implies $\lambda(0) < 1$.

An interesting one parameter family is obtained by setting $a = 0$. It follows from (24) that $\lambda(0) = 2b^2 - 1$. Therefore, we obtain a well with $\lambda(x) > 0$, for $\sqrt{\frac{1}{2}} < b < 1$, whereas for $b > 1$ this is a barrier. This one-parameter family is an example of a pure well or barrier, respectively, because the only extremum of $\lambda(x)$ is at $x = 0$.

Fixing the value of $\lambda(0) = h$ and b gives a cubic equation for a, which is most conveniently expressed in terms of the variable $a + b$, namely

$$(a+b)^3 - \frac{h}{2}(a+b) - \frac{b}{2} = 0\,. \tag{26}$$

This cubic has the discriminant

$$D = -\frac{h^3}{216} + \frac{b^2}{16}\,. \tag{27}$$

Hence equation (26) has three real solutions for $D < 0$, two real solutions for $D = 0$ and only one real solution for $D > 0$. However, not all solutions will lead to regular wells.

In order to gain a better understanding of the various wells and barriers it is useful to calculate

$$\lim_{x\to 0} \frac{d^2\lambda(x)}{dx^2} = \frac{-12(a+b)^6 + 12b(a+b)^3 - b(a+b) + b^2}{2(a+b)^2}\,. \tag{28}$$

When this limit vanishes we have a quartic well.

In figure 1, we considered wells with $\lambda(0) = \frac{1}{4}$. There is a one-parameter family of wells with humps on both sides for $a < 0$. Our main example is $a = -0.25$ and $b = 1.126166088$. There is another one parameter family of wells with $a > 0$ which includes pure wells, the quartic well and double wells. As can be seen in figure 1, the pure wells for $a > 0$ are wider than the pure well at $a = 0$. Using equation (28) we can derive the values for the quartic well, namely, $a = \frac{5\sqrt{5}}{32}$ and $b = \frac{3\sqrt{5}}{32}$ with $\lambda(0) = \frac{1}{4}$. For $a > \frac{5\sqrt{5}}{32}$ we obtain double wells, where there is a local maximum at $x = 0$, and global minima at either side.

In figure 2, we show interesting examples of barriers. Again, there are pure barriers, barriers with wells at either side and volcano (or double peak) barriers.

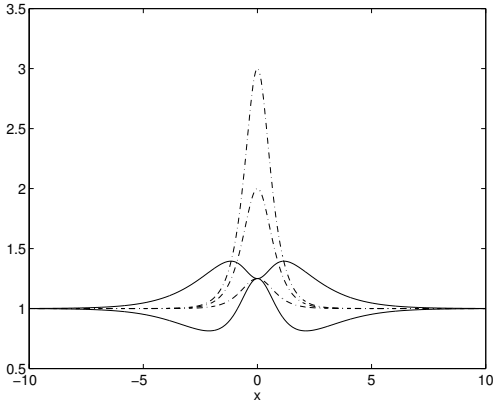

Fig. 2. Different types of barriers: a barrier with two side wells ($a = 0.25$, $b = 0.75$), a volcano barrier ($a = -0.5$, $b = 1.657970214$), and three pure barriers ($a = 0$, $b = \frac{3\sqrt{2}}{4}$), ($a = 0$, $b = \frac{\sqrt{6}}{2}$) and ($a = 0$, $b = \sqrt{2}$) with height 1.25, 2 and 3, respectively.

4. Dynamics of one kink in the presence of wells and barriers

In this section, we consider a sine-Gordon kink travelling towards our standard well with various initial velocities and plot the trajectories. We also calculate the critical velocities for different barriers and compare these to an analytic approximation. First, we briefly comment on our numerical scheme.

The equations of motion for the kinks have been solved using a standard fourth order Runge–Kutta method with gridsize 10001. Plus and minus "infinity" are located at 50 and -50, respectively, so that the stepsize in space is $\Delta x = 0.01$. The stepsize in time has usually been taken to be $\Delta t = 0.0001$ which is the same choice of parameters as in [11]. For small initial velocities of the kink, larger values of Δt are appropriate.

4.1. Plots of trajectories

Figure 3 illustrates all relevant phenomena for one kink interacting with a well. We have chosen the well with parameters $a = -0.25$ and $b = 1.126166088$, which has a minimum $\lambda(0) = \frac{1}{4}$ and two humps at $x \approx \pm 2.20$ of height 1.16.

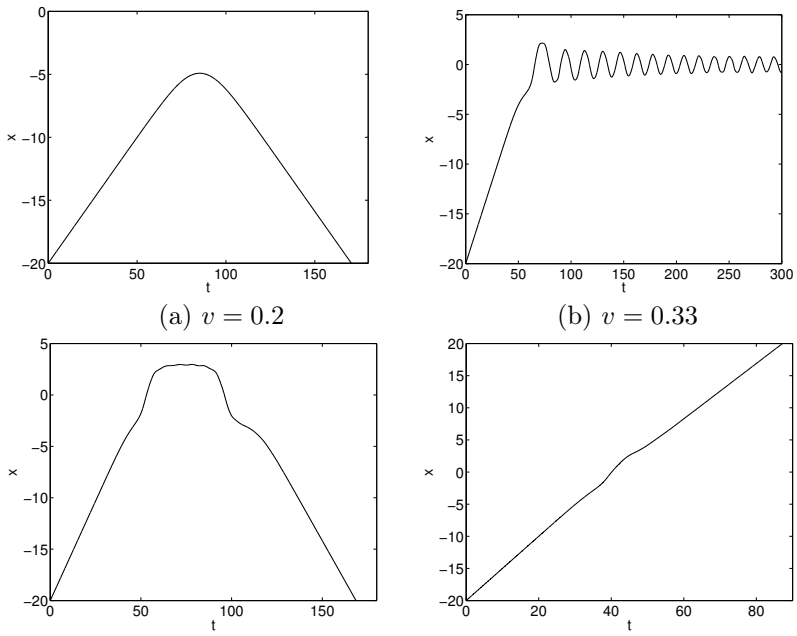

(a) $v = 0.2$ (b) $v = 0.33$

(c) $v = 0.3873$ (d) $v = 0.5$

Fig. 3. Kink trajectories $x(t)$ for a well with $a = -0.25$ and $b = 1.126166088$. (a) shows elastic back-reflection. In (b) the kink becomes trapped in the well. In (c) the kink is back-reflected by the well. In (d) the kink crosses the well.

For low velocity $v < 0.3$, there is elastic back-reflection from the first hump, so that initial and final velocity are equal in size, as in figure 3(a). For higher velocity the kink overcomes the initial barrier and becomes trapped in the well which is illustrated in figure 3(b). The critical velocity u_c is defined as the smallest initial velocity which allows the kink to cross the well (or barrier). For the well discussed here, the critical velocity is $u_c \approx 0.387$. An example of a kink crossing the well is given in figure 3(d), where it can be seen that the kink gains speed inside the well. The most interesting behaviour happens for a narrow range of velocities just below u_c. As figure 3(c) shows, the kink may enter the well, get reflected from the well and then leave the well travelling in the opposite direction. This type of behaviour has been discussed in detail in [11]. For our standard well, these resonance windows are very narrow. In fact the kink in figure 3(c) is trapped for $v = 0.38735$, is back-reflected for $v = 0.38736$ and trapped once more for $v = 0.38737$. For $v = 0.38738$ the kink escapes.

4.2. Critical velocities for one kink interacting with a barrier

In this section we follow an argument in [15] to calculate an analytic approximation to the critical velocity, u_c. We then compare the analytic calculations with numerical results. Finally, we briefly discuss how to apply the moduli space approximation in this context.

The total energy of a kink configuration is given by sum of kinetic and potential energy, namely,

$$E_{\text{total}} = \int_{-\infty}^{\infty} \left(\frac{1}{2} \left(\frac{\partial \phi}{\partial t} \right)^2 + \frac{1}{2} \left(\frac{\partial \phi}{\partial x} \right)^2 + \lambda (1 - \cos \phi) \right) dx \,. \tag{29}$$

Far away from the well, $\lambda \approx 1$, and a kink travelling with speed v is given by equation (9) with total energy

$$E_1(v) = \frac{8}{\sqrt{1 - v^2}} \,. \tag{30}$$

By construction, we know that the kink (15) is a static configuration when the coupling constant λ is given by (16). We first consider the case $a = 0$, then the total energy is given by

$$E_2(b) = \int_{-\infty}^{\infty} \left(\frac{2(b^2 - 1 + 2b^2 \cosh(x)^2)}{b^4 \cosh(x)^4 - 2b^2 (b^2 - 1) \cosh(x)^2 + (b^2 - 1)^2} \right) dx \,. \tag{31}$$

The energy $E_2(b)$ can be evaluated explicitly, but the expression is lengthy. $E_2(b)$ is a monotonically increasing function of b with $E_2\left(\sqrt{\frac{1}{2}}\right) = \sqrt{2}\ln\left(\sqrt{2}-1\right)+6 \approx 4.75$, $E_2(1) = 8$, so that $E_2 > 8$ for $b > 1$ (barrier) and $E_2 < 8$ for $b < 1$ (well).

The critical velocity u_c is the smallest velocity such that the kink passes the obstacle. In the case of elastic scattering, the critical velocity can be evaluated using the conservation of energy, that is by setting

$$E_1(u_c) = E_2(b)\,, \tag{32}$$

as was pointed out in [14]. Since $E_1(v) \geq 8$ this approach is only valid for barriers. For non-zero a the situation is similar, only now there is a larger variety of possible shapes, see figure 2.

In Table I we present critical velocities for kinks interacting with the barriers displayed in figure 2. The critical velocities have been calculated both numerically and using equation (32). It is clear that the theoretical approach is accurate for barriers that are monotonically increasing before the origin and monotonically decreasing afterwards. Otherwise, there is discrepancy, and hence the assumption of elastic scattering is not valid in these cases.

TABLE I

The values of a and b are the parameters of the barriers discussed in figure 2. The column "mass" gives the energy of the a kink located on top of the barrier, the two columns with u_c compare the analytic approximation to the critical velocity to its numerical value, $\lambda(0)$ is the height of the barrier at $x = 0$ and the final column gives the type of barrier.

a	b	Mass	u_c (theoretical)	u_c (numerical)	$\lambda(0)$	Type of barrier
0.25	0.75	8.33	0.271	0.280	1.25	Barrier with wells
−0.50	1.66	9.17	0.489	0.505	1.25	Volcano
0.00	1.06	8.64	0.379	0.379	1.25	Pure barrier
0.00	1.22	10.35	0.635	0.636	2.00	Pure barrier
0.00	1.41	12.28	0.759	0.762	3.00	Pure barrier

In the following, we sketch how we might be able to calculate critical velocities in the case of inelastic scattering. We begin by discussing the moduli space approximation [24], in the context of kinks interacting with wells and barriers. Originally, this method was developed for BPS monopoles where the static solutions of the field equations are a finite dimensional manifold, and relativistic dynamics can be approximated for low velocities as geodesic flow on this manifold. For a single kink with $\lambda = 1$ the moduli space is one-dimensional, generated by translating the kink. For non-constant λ,

the only static solutions are the kink and the antikink. Therefore, we need to include low energy configurations, which are not static, in order to obtain a finite dimensional "moduli space". For the well given by (16) we can choose the following finite dimensional parametrisation of the kink configuration,

$$\begin{aligned}\phi(x,t) &= \pi + 2\arctan\left(A(t)\left(x - X(t)\right) + B(t)\sinh\left(\gamma(t)\left(x - X(t)\right)\right)\right) \\ &\quad + W(t)\phi_{\text{well}}(x)\,. \end{aligned} \tag{33}$$

The time-dependence of the kink is captured by the functions $A(t)$, $B(t)$, $\gamma(t)$, $X(t)$ and $W(t)$ which are coordinates on the moduli space. Here $A(t)$ and $B(t)$ describe how the presence of the well deforms the kink. For low energy configurations, a kink which is static in the well has $A = a$ and $B = b$ whereas a kink far away from the well will have $A \approx 0$ and $B \approx 1$. The parameter $X(t)$ gives the position of the kink and the gamma factor $\gamma(t)$ describes how the kink deforms for high velocities, which has already been discussed in [11]. Finally, $\phi_{\text{well}}(x)$ parametrizes a bound state which arises unless $\lambda(x) \geq 1$ for all x. In order to include multikinks, we could add another kink to (33) with new parameters $\tilde{A}(t)$, $\tilde{B}(t)$, $\tilde{\gamma}(t)$ and $\tilde{X}(t)$, which is a reasonable approximation provided the two kinks are far apart from each other, namely $|X(t) - \tilde{X}(t)| \gg 0$, see [25] for a detailed study in the case $\lambda \equiv 1$.

To simplify the discussion we only consider the case of a pure barrier with $a = 0$ and $b > 1$. In this case, the ansatz (33) reduces to

$$\phi(x,t) = \pi + 2\arctan\left(B(t)\sinh((x - X(t)))\right) \tag{34}$$

assuming low enough speeds, so that the gamma factor can be ignored. Inserting the ansatz into the Lagrangian (1) and integrating over space, we obtain the reduced Lagrangian

$$L = C_1\dot{X}^2 + C_2\dot{B}^2 - V(b,B,X)\,, \tag{35}$$

where

$$C_1 = \frac{2B^2\arctan\sqrt{B^2-1} + 2\sqrt{B^2-1}}{\sqrt{B^2-1}}\,, \tag{36}$$

$$C_2 = \frac{2B^2\arctan\sqrt{B^2-1} - 2\sqrt{B^2-1}}{B^2\sqrt{B^2-1}^3} \tag{37}$$

and $V(b,B,X)$ is a complicated, but explicitly known function of the well parameter b and the kink parameters B and X. For large $|X|$ the reduced potential can be written as

$$V(b,B,X) = U(B) + O\left(\exp\left(-2|X|\right)\right)\,, \tag{38}$$

where $U(B)$ is independent of the well parameter b. For $B \approx 1$, we obtain

$$U(B) = 8 + \tfrac{32}{15}(B-1)^2 + O\left((B-1)^3\right). \tag{39}$$

Hence, for small energies, far away from the well, the kink moves with constant speed and oscillates around the equilibrium configuration $B = 1$. As a useful check, we set $B \equiv 1$, so that $\dot{B} = 0$, to obtain

$$L = 4\dot{X}^2 - 8\,, \tag{40}$$

which is the expected Lagrangian for a free particle of mass 8. This Lagrangian describes geodesic motion on $\mathbb{R}$, the moduli space of a single kink. Note, the geodesic approximation has been rigorously proven by Stuart for vortices and monopoles [26, 27].

A detailed study of the moduli space approximation is beyond the scope of this paper. Here we discussed what kind of parameters may become relevant and gave a partial answer in the case of barriers. For the more interesting case of kinks interacting with wells, a good approximation for the bound mode is required. This is work currently in progress.

5. Dynamics of two kinks in the presence of a well

In general, the interaction of two kinks with a well is rather complicated because the trajectories depend on the initial positions and the initial velocities of both kinks. Here, we restrict our attention to scattering processes when the first kink approaches the well with given initial velocity v, and the second kink is at rest in the well. Our potential $\lambda(x)$ has been chosen, such that the first kink is given asymptotically by equation (9) whereas the second kink is given by equation (15). The exact solution (13) cannot be generalized to our wells. However, since kinks are exponentially localized, we can just concatenate the two kinks provided the first kink is far enough away from the well.

Figure 4 illustrates some important trajectories for our standard well. When the first kink travels with small initial velocity, *e.g.* $v = 0.2$, then there is elastic back-reflection, such that the final velocity of the first kink is $-v$, and the second kink remains at rest in the well, see figure 4(a). The trajectory of the first kink closely resembles the trajectory of a single kink in figure 3(a). Figure 4(b) shows inelastic scattering where the first kink loses energy, and the second kink clearly gains energy because it is now oscillating in the well. In figure 4(c) the second kink is knocked out of the well by the first kink which also escapes from the well. Figure 4(d) shows a similar scenario. The second kink is again knocked out of the well, whereas the first kink is now trapped in the well. It is worth comparing this outcome to the

exact solution when there is no well. In this case, the first kink loses all its kinetic energy to the second kink, so that after the scattering event the first kink is at rest whereas the second kink moves with velocity v.

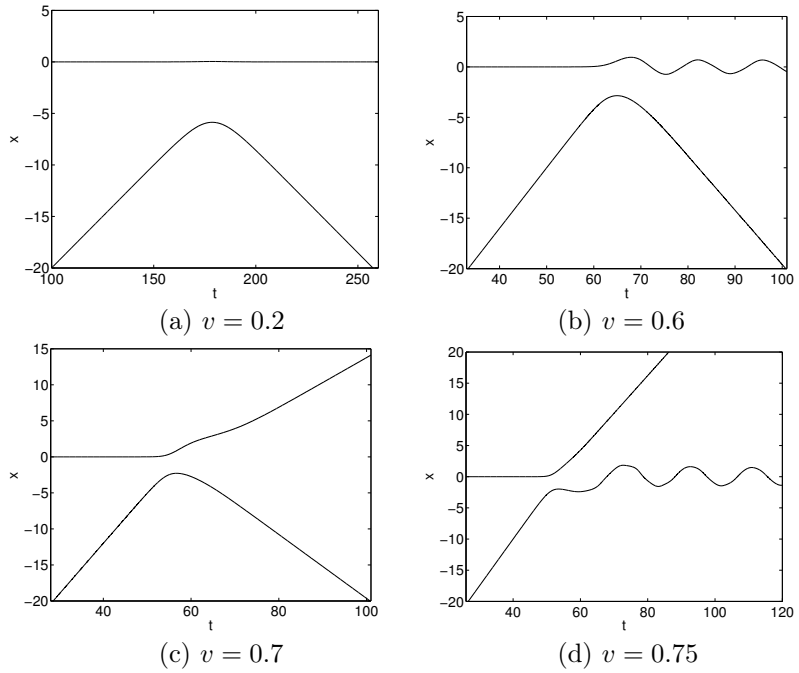

Fig. 4. Kink trajectories $x(t)$ for a well with $a = -0.25$ and $b = 1.126166088$. One kink is travelling towards the well whereas a second kink is stationary inside the well. (a) shows elastic back-reflection, the kink in the well remains stationary. In (b) the kink experiences inelastic scattering, the trapped kink oscillates in the well. In (c) the first kink is back-reflected while the second kink escapes from the well. In (d) the first kink becomes trapped while the second kink escapes from the well.

We checked the range $0.695 < v < 0.6951$ in detail, in the hope that there would be a double back-reflection, so that first kink and second kink both escape on the same side. But for our standard well, we were unable to find this kind of behaviour.

In figure 5, we discuss two interesting trajectories for the quartic well ($a = \frac{5\sqrt{5}}{32}$, $b = \frac{3\sqrt{5}}{32}$). This is a rather wide well which allows both kinks to be trapped. Figure 5(a) shows an interesting quasi-periodic motion where the two kinks knock each other out of the centre of the well but do not gain enough energy to leave the well. Figure 5(b) shows a novel type of back-reflection. The first kink enters the well and speeds up, then hits the

second kink and knocks it off the centre of the well. The second kink slows down, returns to the centre and gives the first kink enough kinetic energy to escape the well.

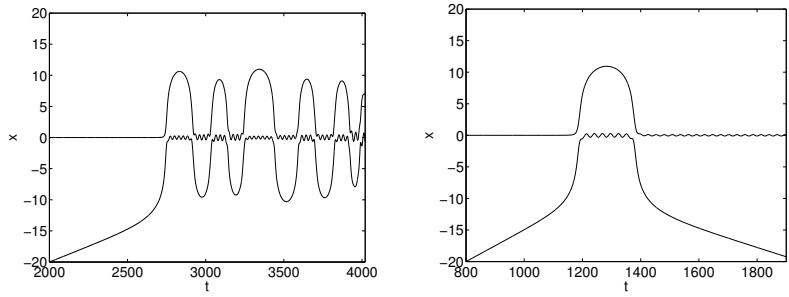

(a) $v = 0.01$ (b) $v = 0.025$

Fig. 5. Kink trajectories $x(t)$ for the quartic well ($a = \frac{5\sqrt{5}}{32}$, $b = \frac{3\sqrt{5}}{32}$). One kink is travelling towards the well with velocity v whereas a second kink is stationary inside the well. In (a) both kinks become trapped in the well. (b) shows a novel type of back-reflection.

Figure 6 shows final *versus* initial velocity for our standard well. In the left figure, one kink travels towards the well with initial velocity v. For $v < 0.3$ the kink is elastically back-reflected. As v is increased, the kink is trapped. For $v > 0.387$ the kink escapes the well. As v tends to one the kink feels the influence of the well less, so that the final velocity tends to the initial velocity for $v \approx 1$. The back-reflection at $v = 0.38736$ is too narrow to be detected with the resolution used for this figure. However, there are additional back-reflections at $v = 0.386$ and $v = 0.381$.

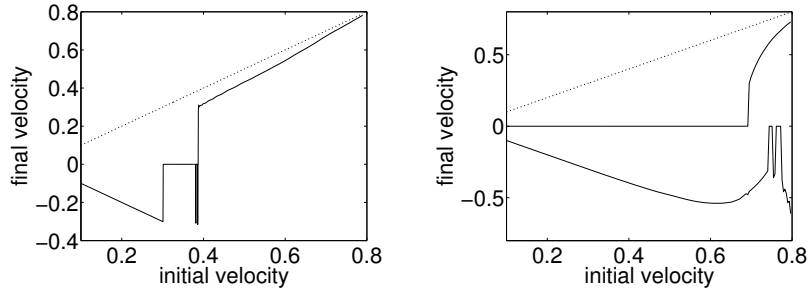

Fig. 6. Final velocity *versus* initial velocity for a kink incident on a well with humps with $a = -0.25$ and $b = 1.126166088$. For the figure on the left, the well is empty whereas for the figure on the right, there is a kink in the well, which is initially at rest. The dotted line corresponds to no obstacle, *i.e.* initial velocity equals final velocity.

The right figure in 6 shows final *versus* initial velocity for our standard well, where a second kink is at rest inside the well. Elastic scattering takes place for a longer range of initial velocity v. As the initial velocity of the incoming kink increases, the kink in the well is set oscillating more energetically. Because of this, at some point the final velocity of the first kink starts to become less negative. At higher initial velocities the final velocity of the initially static kink increases and approaches one, while the final velocity of the other soliton takes the value zero in two separated windows, but is more negative between and after these windows.

Figure 7 shows final velocity *versus* initial velocity for a narrow well without humps. In the left figure, one kink travels towards the well with initial velocity v. There is a series of resonance windows at $v \approx 0.2$ where back-reflections occur. In comparison to figure 6 the behaviour near the critical velocity is less abrupt and back-reflections take place more frequently. For large initial speed, the initial velocity approaches the final velocity. However, there is a region where the curve appears to wobble. In terms of our numerical simulations, we have checked sensitivity to stepsize in time and space independently. The wobble is more sensitive to the stepsize in space, but appears to be a genuine phenomenon. This could be a novel feature due to our potential.

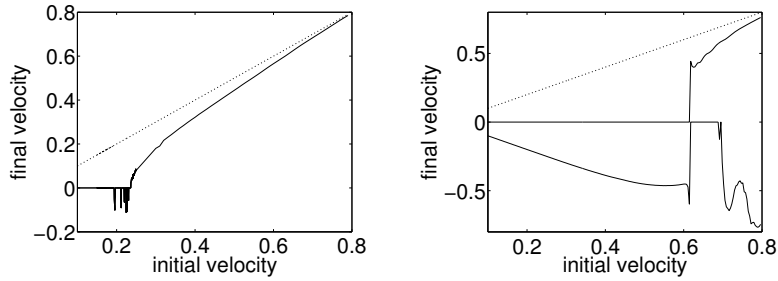

Fig. 7. Final velocity *versus* initial velocity for a kink incident on a narrow well without humps with $a = 0$ and $b = \sqrt{10}/4$. For the figure on the left, the well is empty whereas for the figure on the right, there is a kink in the well, which is initially at rest. The dotted line corresponds to no obstacle, *i.e.* initial velocity equals final velocity.

The figure on the right in 7 shows final velocity *versus* initial velocity for the narrow well without humps, where a second kink is initially static in the well. At small to medium initial velocities, elastic and inelastic back-reflections occur. For velocity $v > 0.6$ the static kink is ejected from the well and at marginally greater initial velocity, the first kink becomes trapped. For higher velocities both kinks escape the well in opposite directions. Again, the final velocity of the first kink is not a monotonic function of the initial velocity.

6. Conclusion

In this paper, we have discussed the interactions of kinks with wells and barriers. We introduced a novel class of smooth potentials which include pure wells and pure barriers of various heights and widths. These potentials also give rise to wells with two side barriers and barriers with two side wells, as well as double wells and volcano barriers. The main advantage of the proposed potentials is that the static kink-in-the-well solution is explicitly known. The asymptotic kink solution for a kink located at very large X is also known. Therefore, a kink can be scattered off a kink-in-the-well and the only relevant parameter is the initial velocity of the incoming kink. When the exact solution of the kink in the well is not known, then the trapped kink tends to oscillate in the well, such that the scattering behaviour depends not only on the velocity of the incoming kink but also on the phase of the trapped kink, which is more difficult to control.

We studied the scattering of one kink off a well, mainly focussing on our standard well with $\lambda(0) = \frac{1}{4}$ and two side humps, and reproduced all the known phenomena such as trapping, back-reflection and escape. We then compared numerically calculated critical velocities for various barriers to an analytic approximation assuming elastic scattering. As expected, there was good agreement for pure barriers, and less agreement for the volcano barrier and the barrier with side wells.

The novel feature of this paper is the scattering of multi-kinks in the presence of a well. We calculated various trajectories for our standard well, such as elastic scattering, inelastic scattering, kink one replacing kink two in the well and a scattering where both kinks escape. Unfortunately, we were unable to find a double back-reflection for our standard well, but it is likely that such a trajectory exists for the right choice of well parameters and initial velocity. For the quartic well, we found double trapping of kinks and a novel type of back-reflection. We also plotted initial velocity against final velocity, both for an empty well and a kink trapped in a well. In the case of our standard well with humps, we found that, for a single kink, the plot reproduced all the expected behaviour. In the case of an incoming kink and a kink initially in the well we found for small to medium initial velocities there are back-reflections that start off as elastic then become inelastic. When the initial velocity becomes high, the static kink is ejected and there are two windows in which the initially moving kink is trapped. For a narrow well without humps the plot for a single kink revealed resonance windows and an interesting wobbling behaviour. The plots for two kinks showed that as the initial velocity increases, there is a point where the static kink is ejected and further on, the first kink becomes trapped. At high speeds both kinks escape the well, moving in opposite directions. Again, the final velocity of the first kink is not a monotonic function of the initial velocity.

A long term aim of this line of work is to be able to design wells which have desirable properties. In certain physical systems, it is possible to make the coupling constant inhomogeneous, *e.g.* the ferromagnetic spin chain described in the introduction [5]. Barriers and wells might then be used to control kink dynamics, for example, by acting as filters. An even more ambitious aim is discussed in [28] where a particular kind of integrable point defect could be used to construct simple logical gates.

Our approach is applicable to various different systems. The $\lambda\phi^4$ kink allows similar wells and barriers which would enable the study of kink–antikink scattering in the presence of barriers and wells. Note that kink–antikink scattering is a fascinating subject which leads to interesting resonance structures, see *e.g.* [29] for $\lambda\phi^4$ and [30] for related solitons. Soliton-well interaction has also been discussed for various other solitons, for example, deformed sine-Gordon models [13, 31], $\lambda\phi^4$ models [12], Q-ball systems [14] or generalized sigma models [16] where our approach may again prove to be useful.

Reference [25] presents calculations for two interacting kinks using the method of Manton for constant λ. In [11] a moduli space approximation was proposed which also takes account of the degrees of freedom of the well. See [20] for related work on the $\lambda\phi^4$ kink. In Section 4.2 we described how to apply the moduli space approximation in our case. Our calculations imply that the an additional degree of freedom could be the slope of the soliton at the centre of the kink as parametrized by a and b. One could therefore investigate moduli space dynamics applied to the model described in this paper, where a, b and X for each kink become functions of time t, and the degree of freedom of the well is also taken into account. This is currently work in progress.

S.W.G. is grateful to Giota Adamopoulou for helpful conversations about physical interpretations of this work. Thanks go to Andy Hone for discussions and comments at various stages of the project. S.K. and R.H. acknowledge the Nuffield Foundation for a Nuffield Science Bursary. S.W.G. is supported by the EPSRC (EP/P503388/1) and by the SMSAS, University of Kent.

REFERENCES

[1] N. Manton, P. Sutcliffe, *Topological Solitons*, University Press, Cambridge, UK, 2004.

[2] B.D. Josephson, *Rev. Mod. Phys.* **46**, 251 (1974).

[3] J.K. Perring, T.H.R. Skyrme, *Nucl. Phys.* **31**, 550 (1962).

[4] S. McCall, E.L. Hahn, *Phys. Rev.* **183**, 457 (1969).

[5] G. Wysin, A.R. Bishop, P. Kumar, *J. Phys. C: Solid State Phys.* **17**, 5975 (1984).

[6] E. Abdalla, B. Maroufia, B.C. Melgar, M.B. Sedra, *Phys. A: Stat. Mech. Appl.* **301**, 169 (1984).

[7] Z. Fei, Y.S. Kivshar, L. Vazquez, *Phys. Rev.* **A45**, 6019 (1992).

[8] R.H. Goodman, R. Haberman, *Physica D* **195**, 303 (2004).

[9] B.A. Malomed, A.A. Nepomnyashchy, *Phys. Rev.* **B45**, 12435 (1992).

[10] Y.S. Kivshar, B.A. Malomed, *Rev. Mod. Phys.* **61**, 763 (1989).

[11] B. Piette, W.J. Zakrzewski, *J. Phys.* **A40**, 5995 (2007) [arXiv:hep-th/0611040v1].

[12] J.H. Al-Alawi, W.J. Zakrzewski, *J. Phys.* **A40**, 11319 (2007) [arXiv:0706.1014v1 [hep-th]].

[13] J.H. Al-Alawi, W.J. Zakrzewski, *J. Phys.* **A41**, 315206 (2008) [arXiv:0802.1939v1 [hep-th]].

[14] J.H. Al-Alawi, W.J. Zakrzewski, *J. Phys.* **A42**, 245201 (2009) [arXiv:0902.4358v1 [math-ph]].

[15] J.H. Al-Alawi, arXiv:0911.1804v1 [hep-th].

[16] L.A. Ferreira, B. Piette, W.J. Zakrzewski, *J. Phys. Conf. Ser.* **128**, 012027 (2008) [arXiv:0709.3919 [hep-th]].

[17] L.A. Ferreira, B. Piette, W.J. Zakrzewski, *Phys. Rev.* **E77**, 036613 (2008) [arXiv:0708.1088 [hep-th]].

[18] B. Piette, W.J. Zakrzewski, J. Brand, *J. Phys.* **A38**, 10403 (2005) [arXiv:hep-th/0508032].

[19] K. Javidan, *J. Phys.* **A39**, 10565 (2006).

[20] G. Kalbermann, arXiv:hep-th/9805169v1.

[21] A. Scott, *Nonlinear Science*, Oxford University Press, Oxford 1999.

[22] M.J. Ablowitz, P.A. Clarkson, *Solitons, Nonlinear Evolution Equations and Inverse Scattering*, London Mathematical Society Lecture Note Series vol. 149, Cambridge University Press, Cambridge 1991.

[23] G. Kalbermann, *J. Phys.* **A37**, 11603 (2004) [arXiv:cond-mat/0408198v2 [cond-mat.other]].

[24] N.S. Manton, *Phys. Lett.* **B110**, 54 (1982).

[25] P.M. Sutcliffe, *Nucl. Phys.* **B393**, 211 (1993).

[26] D. Stuart, *Commun. Math. Phys.* **159**, 51 (1994).

[27] D. Stuart, *Commun. Math. Phys.* **166**, 149 (1994).

[28] E. Corrigan, C. Zambon, *J. Phys.* **A37**, L471 (2004) [arXiv:hep-th/0407199v1].

[29] D.K. Campbell, J.F. Schonfeld, C.A. Wingate, *Physica D* **9**, 1 (1983).

[30] D.K. Campbell, M. Peyrard, *Physica D* **18**, 47 (1986).

[31] D. Bazeia, L. Losano, J.M. C. Malbouisson, R. Menezes, *Physica D* **237**, 937 (2008) [arXiv:0708.1740v2 [nlin.PS]].